Synthesis and characterization of silica nanoparticles with modified surface for hydrophobic coatings

TEODORA MĂLĂERU[1], MIRELA MARIA CODESCU[1], ELENA CHIȚANU[1,*], GABRIELA GEORGESCU[1], CRISTINA ANTONELA BANCIU[1,*], RADU CRISTIAN DASCĂLU[1], DELIA PĂTROI[1], VIRGIL MARINESCU[1], ISTVAN BORBATH[2]

[1]*National Institute for Research and Development in Electrical Engineering ICPE-CA Bucharest, 313 Splaiul Unirii, 030138, Bucharest 3, Romania*

[2]*SC Roseal SA, 5/A N. Balcescu St., 535600, Odorheiu Secuiesc, Harghita, Romania*

The paper presents the synthesis of spherical silica nanoparticles with narrow particle size distribution by a PVP surfactant-assisted sol-gel process and the modification of their surface character through a post-grafting process with a silane (PFOTS). X-ray diffraction, FT-IR spectrometry and EDS compositional analysis confirm the formation of silica structures and the presence of the silane layer on their surface. The hydrophobic character was tested by measuring the water contact angle. The resulting value of 148° supports the change in the character of their surface from hydrophilic to hydrophobic.

(Received June 24, 2021; accepted February 11, 2022)

Keywords: Silica nanoparticles, Sol-gel, Hydrophobicity, Silane

1. Introduction

Nanotechnology has seen an explosive development in the last decade because of the progress in the field of materials engineering. Thus, different nanoparticles with specific properties and functions for their applications are designed to have the shape, size, and surface controlled at the nanoscale. Among the many nanoparticles, silica nanoparticles have seen an increased demand for applications in catalysis [1, 2], electronics [3], photonics [4, 5], biotechnology [6], drug transport [7] and to improve the surface and mechanical properties of materials such synthetic rubber and resins [8]. Thus, for the realization of silica nanoparticles suitable for a wide range of applications, additional research was needed in terms of synthesis methods and techniques.

In 1956, Gerhard Kolbe [9] observed the formation of spherical particles from tetraethyl orthosilicate (TEOS) in ethanol, as solvent, and in the presence of ammonia, as catalyst, and afterwards Werner Stöber [10] improved the precipitation procedure. Since then, many methods for the synthesis of silica nanoparticles have been developed such as sol-gel [11, 12], microemulsion [13], hydrothermal techniques [14, 15], combustion [16] and pyrolysis synthesis [17]. Among them, the sol-gel method, a simple and efficient method for the synthesis of controlled-size silica nanoparticles, has been intensively exploited and developed. Zulfiqar and collaborators [18] reported the obtaining of silica nanoparticles with spherical shape and controlled size by modifying the ratio between ammonia and ethanol using sodium silicate diluted with distilled water as a precursor. Also, in another research [19], the preparation of ultrafine (50-55 nm) silica nanoparticles using the alkoxide route of the sol-gel method was reported, in which tetraethoxysilane (TEOS) was used as a precursor and hydrochloric acid (HCl) as a catalyst. Disperse amorphous SiO_2 nanoparticles were also prepared through a simple sol-gel method in which PEG 1000 was used as surfactant [20].

Numerous studies have shown that the silica nanoparticles thus prepared have a hydrophilic surface due to the presence of polar hydroxyl (-OH) groups. These groups (-OH) exist on the surface of silica nanoparticles in various forms such as (≡Si-OH) isolated silanol, (≡$Si(OH)_2$) geminal silanol or vicinal silanol in which the (-OH) group bind to each other by hydrogen bonds [21]. Therefore, it is necessary to functionalize the silica nanoparticles in order to give them a hydrophobic character and therefore increase the compatibility between silica and different materials such as paint, synthetic rubber, resin, adhesive, etc. To date, several studies have been performed to treat the surface of silica nanoparticles following the selection of the optimal reagent and the modification procedure. The main objective of this study was to prepare spherical silica nanoparticles (SN) with narrow particle size distribution by a modified surfactant-assisted sol-gel process and to modify their hydrophilic surface in the hydrophobic surface by a post-grafting process with PFOTS.

Superhydrophobic surfaces are of particular interest, because it is expected to obtain some properties such as: anti-contamination, self-cleaning, anti-wetting, anti-corrosion, anti-freeze, and extending the life of products. These properties are attractive for many industrial and biological applications, such as: dirt-repellent paints for naval ships, deicing of aircraft wings or wind turbine, antennas and windows with a protective layer to prevent snow deposition, hydrophobic treated bottles for traffic lights or other traffic control units, anti-rain windshields, anti-fog coatings, anti-fog glasses, microfluidic devices, metal refining, dirt-repellent architectural coatings [22,23,24].

2. Experimental

2.1. Materials

Tetraethylortho-silicate (TEOS) (98%), purchased from ACROS ORGANICS, ethylenediamine from VWR CHEMICALS, and polyvinylpyrrolidone (PVP) having molecular weight 40000 g/mol from SIGMA-ALDRICH were used as reagents. Ethyl alcohol absolute (99,9%) from MERCK was used as solvent, 1H,1H,2H,2H-perfluorooctyltriethoxysilane (PFOTS) (97%) from Alfa Aesar as a coupling agent, hydrochloric acid (HCl) 1N purchased from MERCK and deionized ultrapure water (D.I. H_2O), which was obtained from Millipore Simplicity – UV equipment for washing and purification.

2.2. Synthesis of silica nanoparticles

25 mmol of TEOS was added to 150 ml of ethyl alcohol and stirred under sonication for 15 minutes at room temperature. Then, a volume of 5 ml D.I. H_2O was added dropwise to the mixture of TEOS and ethyl alcohol and mixed under sonication for another 15 minutes at room temperature. To the reaction mixture thus formed 15 ml ethylenediamine as a catalyst and gelling agent and 2 ml of a 4% aqueous solution of PVP as surfactant were added and mixed again for another 15 minutes under sonication at room temperature.

The resulting reaction mixture was left to gel and complete the reaction overnight at room temperature. The obtained white precipitate was washed twice with D.I. H_2O and finally with absolute ethyl alcohol and separated from the residual mixture by centrifugation at 4000 rpm for 15 minutes. After separation, the solid part was dried in an oven at 80°C for 6 h. The resulting white powder was then milled in a mortar for characterization and on the other hand for further processing for functionalization of the surface of nanoparticles with the silane (PFOTS).

2.3. Modification of SN surface by post-grafting process with PFOTS

0.1 g of SN thus prepared were dispersed by stirring under sonication at room temperature for 30 minutes, in 20 ml of 9:1 mixture of ethyl alcohol and DI H_2O. The solution pH was adjusted to 1 by dripping 1N HCl. 0.8 μmol of PFOTS which was immediately added to the dispersion thus made and afterwards it was refluxed at 80°C for 12 h. After cooling the reaction mixture to room temperature, the modified silica nanoparticles by grafting with PFOTS were separated by filtration, washed twice with D.I. H_2O and finally with absolute ethyl alcohol and afterwards dried in a vacuum oven at 50 mbar for 10 h.

2.4. Characterization

The X-ray diffraction investigation was performed with using a Bruker-AXS X-ray diffractometer type D8 Discover, the technical analysis conditions being the following: X-ray tube with Cu anode, 40kV / 40 mA, 1D LynxEye detector, angular increment: 0.04°, angular measuring range $2\theta=10^{o}$-100^{o}. Fourier Transform Infrared (FT-IR) spectra of silica nanoparticles were recorded with a PerkinElmer 100 FT-IR spectrometer in the range of 4000-400 cm^{-1} with a resolution of 4 cm^{-1}. The surface morphology and size of SN were observed by FESEM-FIB Scanning Electron Microscope (Workstation Auriga) equipped with a dispersive X-ray spectroscope detector (Oxford Instruments). Elemental compositions were determined by analysing an area through Energy-dispersive X-ray spectroscopy (EDS). The average hydrodynamic diameter and the size distribution of the nanoparticles were determined using the Dynamic Light technique Scattering - DLS by means of a type 90 Plus device (Brookhaven), equipped with a laser with 32 kW output power and 660 nm wavelength, a photodiode detector with avalanche (APD), a TurboCorr data acquisition board type 9000AT, a Peltier module and "BIC Particle Sizing" software. The contact angle was determined using an optical microscope DinoLite Pro, equipped with a camera for capturing images on the computer and through their processing with the help of Image J software, Drop Analysis-Drop Snake function.

3. Results and discussion

3.1. PFOTS grafting mechanism

In the mixture of ethyl alcohol and water, SN adsorb H_2O molecules on their surface and can hydrolyse PFOTS molecules as they approach their surface and create OH groups on PFTOS molecules (Fig. 1).

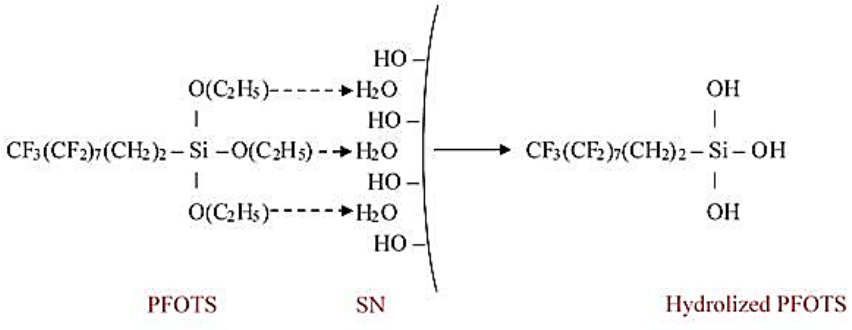

Fig. 1. The hydrolysis of PFOTS molecules (color online)

The hydroxyl (-OH) groups in the hydrolyzed PFOTS structure can react with silanol (Si-OH) groups on the surface of SN by homocondensation, thus creating covalent bonds while other hydroxyl groups can form hydrogen bonds or interact electrostatically with other hydrolyzed PFOTS molecules (Fig. 2).

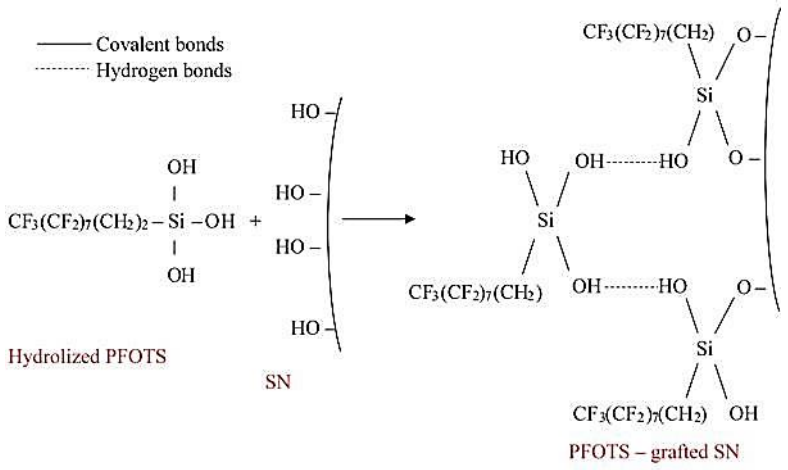

Fig. 2. Homocondensation and physisorbtion of hydrolyzed PFOTS molecules in post-grafting process (color online)

During the washing process, hydrogen bonds and electrostatic interactions are broken due to the high polarity of water molecules. Thus, only the silane molecules covalent bounded remained on the surface of the SN, the excess of the silane being removed by washing [25].

3.2. Structural characterization

The XRD pattern recorded on the sample of SN prepared by the surfactant assisted sol-gel method is shown in Fig. 3. This pattern shows the presence of a single intense peak at 2θ=21.985° which can be assigned to (101) reflection (Sheet ICDD PDF2 00-039-1425) of the silica nanoparticles of amorphous nature. No other impurity peaks were present, which indicates the formation of pure SN.

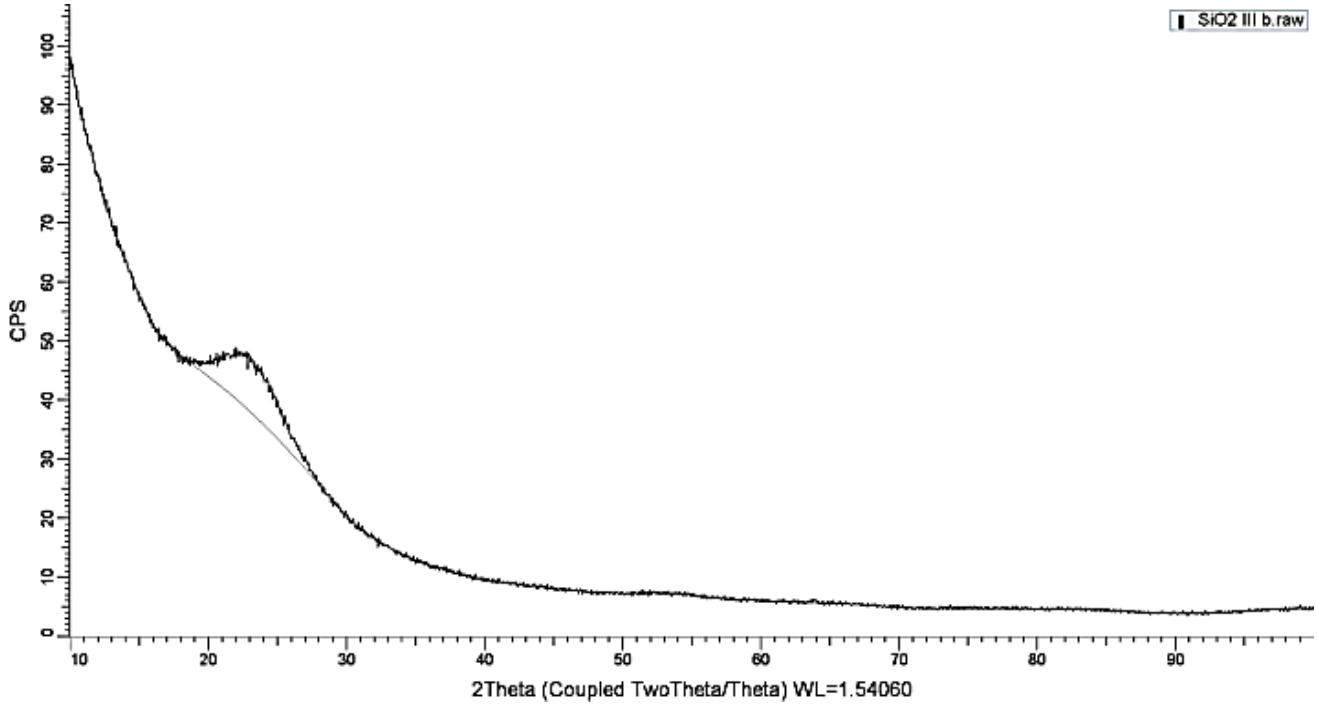

Fig. 3. The XRD pattern recorded on the sample of SN prepared by the surfactant assisted sol-gel method

The structural differences between SN with unmodified surface and those with modified surface through a post-grafting process with PFOTS were investigated by FT-IR spectrometry using KBr method. The FT-IR recorded spectra are shown in Fig. 4 (a-b).

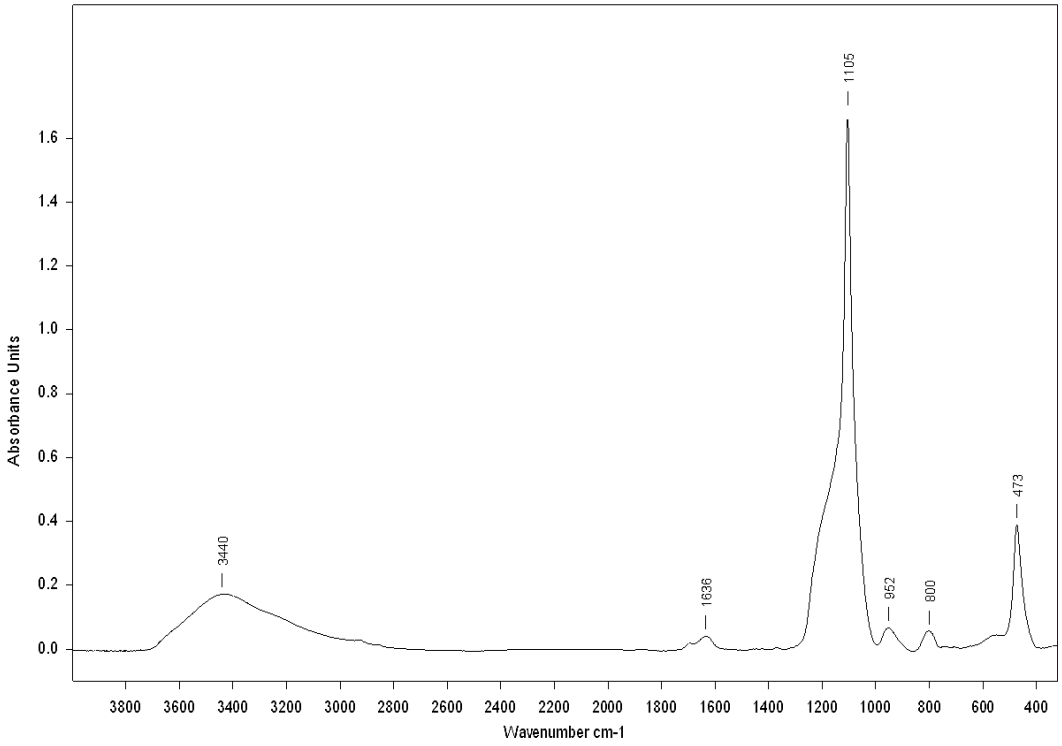

(a)

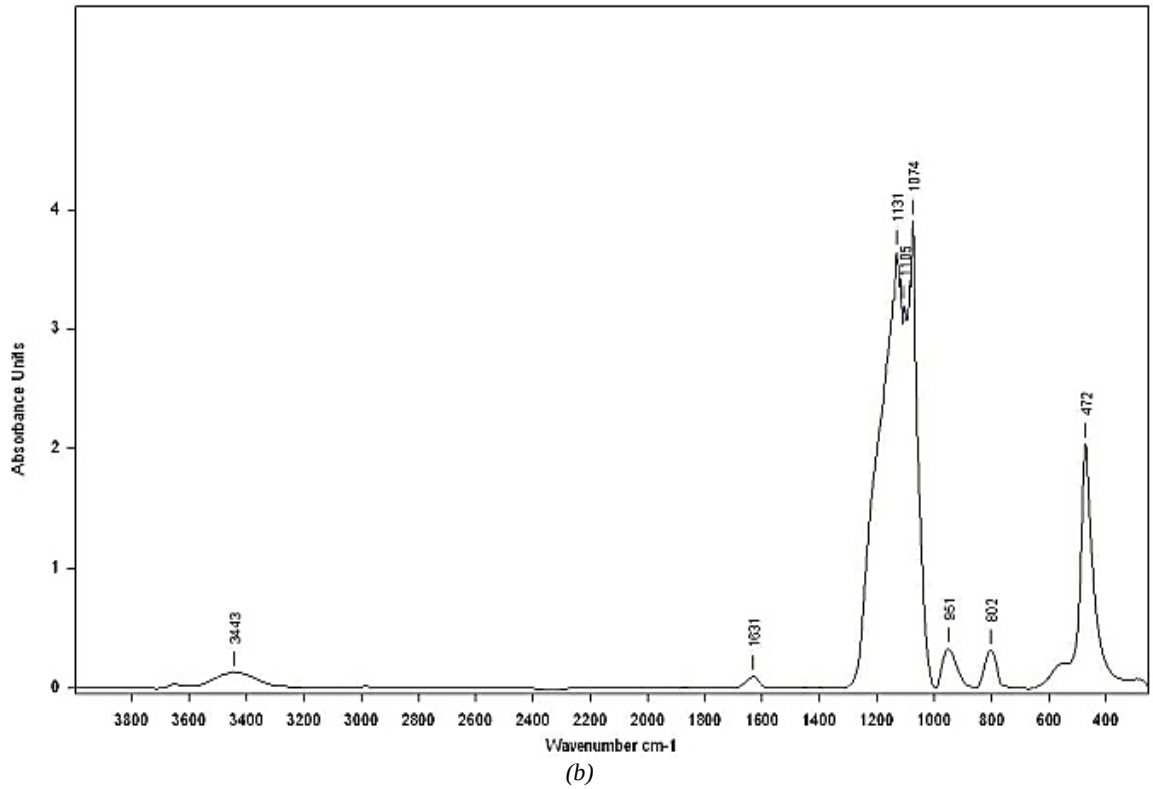

(b)

Fig. 4. FT-IR spectra for (a) SN with unmodified surface and (b) SN with PFOTS modified surface

The FT-IR spectrum recorded on the sample of SN with hydrophobic unmodified surface (Fig. 4 (a)) show the presence of four peaks assigned to bending vibration of Si-O-Si (473 cm^{-1}), to the symmetric stretching vibration of Si-O-Si (800 cm^{-1}), the vibration of external Si-OH groups (952 cm^{-1}) and asymmetric stretching vibration of Si-O-Si (1105 cm^{-1}). The IR spectra also show a low-intensity peak at 1636 cm^{-1} assigned to the H_2O retained on the surface of SN and a peak at 3440 cm^{-1} associated with the stretching of the -OH group [26, 27].

After modifying the surface of SN through the post-grafting process with PFOTS, the silica structure is maintained. The FT-IR spectrum (Fig. 4 (b)) displays the same peaks without major changes at wavelengths of 472 cm^{-1} attributed to the bending vibration of Si-O-Si bonds, to 802 cm^{-1} attributed to the asymmetric stretching vibration of Si-O-Si bonds, at 951 cm^{-1} associated with the vibration of external Si-OH groups. The peak at 1105 cm^{-1} is also present but of higher relative intensity associated with a new intense peak at 1074 cm^{-1} which supports the formation of Si-O-Si bonds by grafting PFOTS on the surface of SN as presented in Fig. 2. In addition, the FT-IR spectrum displays a peak at 1131 cm^{-1} attributed to the stretching vibration of the C-F bonds in the PFOTS structure. In the FT-IR spectrum of Fig. 4 (b) the two peaks from 1631 cm^{-1} and 3443 cm^{-1} respectively are maintained, but they are of much lower intensity, which supports the decrease of the density of Si-OH groups on the surface of SN as a result of the grafting process with PFOTS.

Also, the occurrence of these peaks can be explained by the presence of free lateral silanol groups that originated from the structure of the hydrolyzed silane.

3.3. Morphological and dimensional characterization

Fig. 5 (a) shows SEM image of SN with unmodified surface. This confirms the spherical shape of silica nanoparticles and the absence of irregular particles demonstrated by the control of high uniformity in shape in these synthesis conditions. The average diameter of SN was estimated by sizing a number of particles n=9 from the SEM micrograph and was calculated at a value of 295.34 nm.

The SEM image of SN with surface modified with silane in the post-grafting process (see Fig. 5 (b)) also showed high uniformity of the spherical shape of the nanoparticles. The SN average diameter was determined as being 304.42 nm. The approximately 9 nm larger average diameter of SN with modified surface by grafting with PFOTS compared to that of nanoparticles with unmodified surface was attributed as the thickness of the layer of PFOTS grafted on their surface.

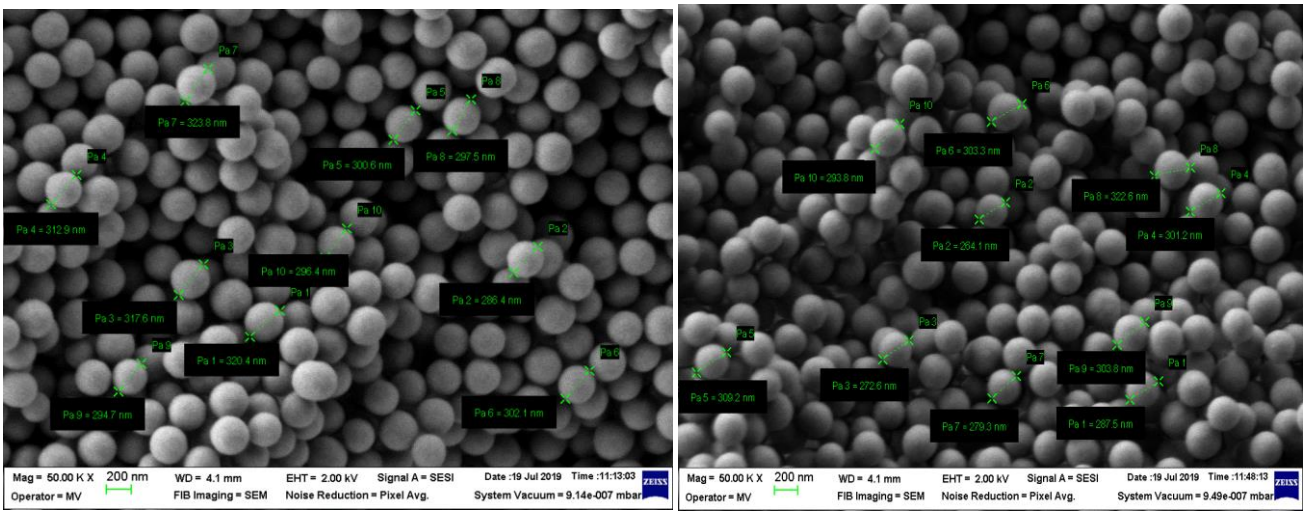

(a) *(b)*

Fig. 5. (a) SEM image of SN with unmodified surface; (b) SEM image of SN with surface modified with PFOTS in the post-grafting process (color online

Average hydrodynamic diameter and size distribution of the nanoparticles obtained by DLS were expressed as a distribution by number, using the cumulative analysis Multimodal Size Distribution (MSD) calculation model. In a DLS analysis, 10 determinations are performed for each test, reporting the value of the average hydrodynamic diameter and the standard deviation. The size distribution profile of silica nanoparticle samples with PFOTS modified surface is presented in Fig. 6.

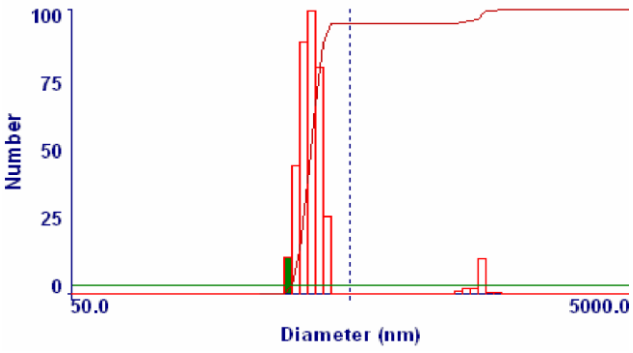

Fig. 6. Average hydrodynamic diameter and the size distribution of the nanoparticles, acquired by DLS, for SN samples with PFOTS modified surface (color online)

The value of mean hydrodynamic diameter and standard deviation relative to number (size distribution multimodal-MSD) is 405±0.027 nm.

3.4. Compositional characterization

The chemical composition of SN with and without surface modified with PFOTS was analysed comparatively by energy dispersive spectroscopy (EDS). The EDS spectrum (Fig. 7 (a)) recorded on the sample of SN with unmodified hydrophobic surface indicates the presence of only the elements Si (44.4 wt. %) and O (56.6 wt. %) in the ratio correspondingly SiO_2 without the presence of other impurities.

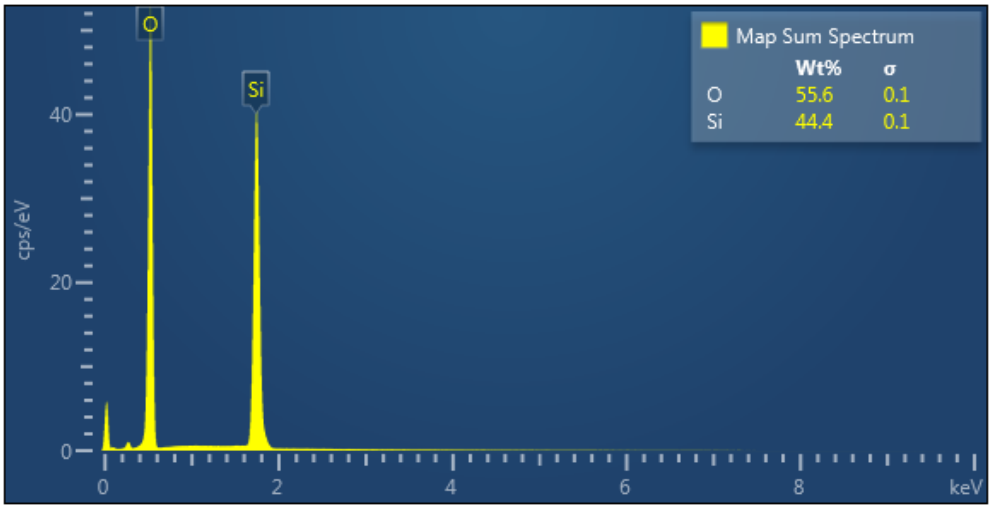

(a)

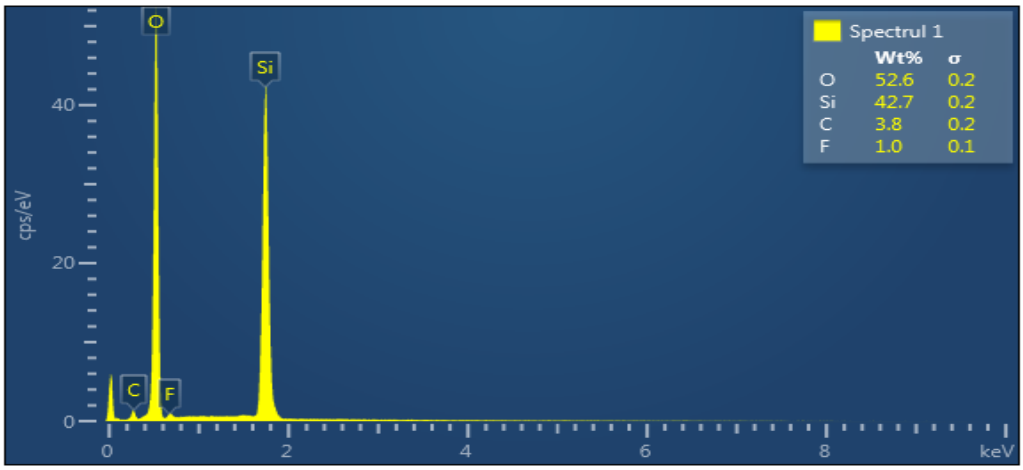

(b)

Fig. 7. The EDS spectra for: (a) SN with unmodified surface; (b) SN with PFOTS surface modified (color online)

For SN with surface modified with PFOTS, the EDS spectrum (Fig. 7 (b)) shows, in addition, the presence of elements C (3.8 wt. %) and F (1 wt. %) elements that are part of the PFOTS structure. The result of the EDS analysis in accordance with the FT-IR analysis supports the formation of the silane layer on the surface of SN by creating covalent bonds following the grafting process.

3.5. Water contact angle (CA)

Evaluation of the SN hydrophobicity with modified surface by grafting with PFOTS was performed by measuring CA using distilled water as wetting agent. The processed image for CA determination is illustrated in Fig. 8 and the results obtained in the determination of CA are presented in Table 1.

The CA value of ~148°, determined for the SN with PFOTS modified surfaces, show the change in the surface character of SN from hydrophilic to hydrophobic due to the fact that most of the -OH groups on the surface were replaced with radicals containing low surface energy chemical groups such as fluorocarbons (-CF_3; -CF_2).

Table 1. Values of CA measured on SN with PFOTS modified surface

Sample	Water contact angle(CA)		
	Left	Right	Mediate
SN with modified surface by grafting with PFTOS	148.434°	148.538°	148.486°

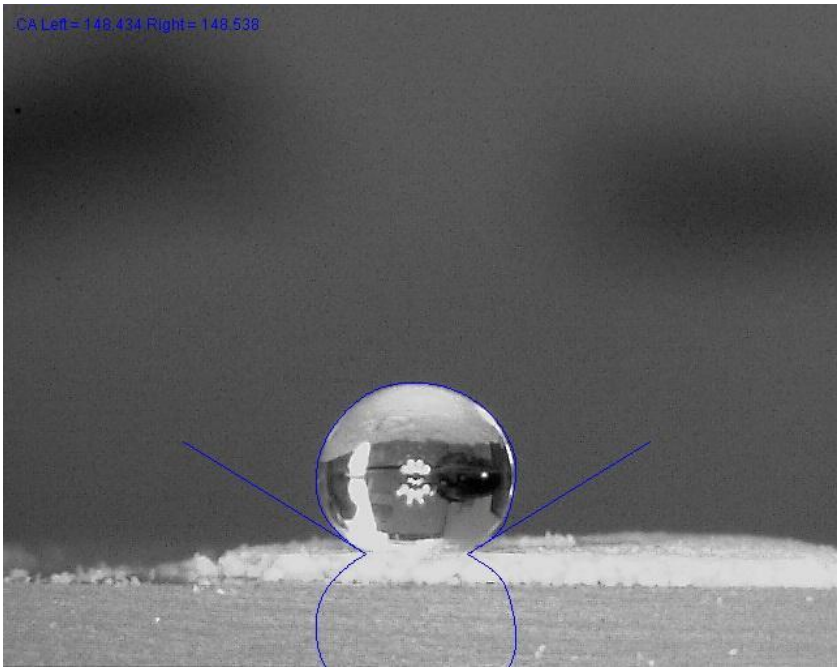

Fig. 8. The processed image for CA determination (color online)

The result of CA measurement is consistent with that of FT-IR and EDS investigations, supporting the grafting of the PFOTS silane to the surface of SN.

4. Conclusions

Hydrophobic modified surface SN with PFOTS were synthesized using PVP surfactant-assisted sol-gel method and a subsequent post-grafting process. The result of the XRD analysis confirmed the formation of silica with an amorphous structure, a result also supported by that of the FT-IR analysis, which in addition highlighted the presence of silanol groups on their surface. In addition, the results of EDS and FT-IR analyses demonstrated the presence of the PFOTS layer on the surface of SNs, through the presence of C and F elements and respectively by forming covalent bonds following the post-grafting process. SEM images showed the formation of spherical nanoparticles with a narrow size distribution of 264-322 nm for nanoparticles with unmodified surface and slightly larger, encompassing the range 286-323 nm, in the case of those with modified graft surface. The result obtained for the water contact angle of 148° confirmed the change in the surface character of SN from hydrophilic to hydrophobic. The good hydrophobic properties developed by PFOTS functionalization of silica nanoparticles recommend them to be used in superhydrophobic surface coatings, for example in the case of wind turbine blades, where are required self-cleaning, water repelling and de-icing properties of the exposed surfaces.

Acknowledgements

This work was supported by the Competitiveness Operational Programme, project no. P_40_403, code My SMIS 105568, subsidiary ctr. no. 133 D4 ROSEAL/2018.

References

[1] J. I. Golea, C. Burda, Z. I. Wang, M. White, J. Phys. Chem. Solids **66**, 546 (2005).

[2] P. Wang, S.M. Zakeeruddin, P. Comte, J. Exmar, M. Grätzel, J. Am. Chem. Soc. **125**(5), 1166 (2003).
[3] H. Gleiter, T. Schimmed, H. Hahn, Nano Today **9**, 17 (2014).
[4] A. Chappini, C. Armellini, A. Chiasers, M. Ferrari, Y. Jestin, M. Mallarelli, M. Montagna, E. Moser, G. N. Conti, S. Pelli, G. C. Reghini, M. C. Goncalves, R. M. Almeida, J. Non. Cryst. Solids **353**, 674 (2007).
[5] R. Wang, H. Zhang, Q. Ma, H. Niu, J. Xu, J. Optoelectron. Adv. M. **22**(1-2), 29 (2020).
[6] Y. Jin, S. Lobstreter, D. T. Pierce, J. Parisien, M. Wu, C. Hali, J. X.-Zhao, Chem. Mater. **20**, 4411 (2008).
[7] M. E. Davis, D. M. Shin, Nat. Rev. Drug Discover **7**(9), 771 (2008).
[8] J. Gao, L. Junting, B. C. Benicewicz, S. Zhao, H. Hillborg, L. S. Schadler, Polymers **4,** 187 (2014).
[9] G. Kolbe, Das Komplexchemische Verhalten der Rieselsäure, dissertation, Jena Univ, (1956).
[10] W. Stöber, A. Fink, E. Bohn, J. Colloid Interface Sci. **26**, 62 (1968).
[11] I. Ab Rahman, V. Padavetton, J. Nanomaterials **2012**, 132424 (2012).
[12] H. N. Azlina, J. N. Hasmidawani, H. Norita, S. N. Surip, Acta Phys. Pol. **129**(4), 842 (2016).
[13] M. A. Malik, M. Y. Wani, M. Ali Hashim, Arab. J. Chem. **5**, 397 (2012).
[14] V. Potapov, R. Fediuk, D. Gorev, Nanomaterials **10**, 624 (2020).
[15] S. S. Taib, M. K. Ahmad, N. Nafarizal, C. F. Soon, N. J. Yaacob, J. Lias, N. M. Ramli, A. B. Suriani, A. Mohamed, M. H. Mamat, M. F. Malek, M. Shimomura, J. Optoelectron. Adv. M. **23**(1-2), 79 (2021).
[16] C. W. Yeh, H. K. Ma, E. Zhao, Combust. Sci. Technol. **173**(1), 25 (2001).
[17] S. R. Almeida, C. Elicker, B. M. Vieira, F. H. Cabral, A. F. Silva, P. J. S. Filho, C. W. Rauback, C. A. Hartwig, M. F. Mesko, M. L. Moreira, S. Cava, Dyes Pigm. **164**, 272 (2019).
[18] U. Zulfiqar, T. Sulohani, S. W. Husain, J. Sol-Gel Sci. Technol. **77**, 753 (2016).
[19] R. Nandanwar, P. Singh, F. Z. Hague, Chemical Science International Journal **5**(1), 1 (2015).
[20] Q. Guo, D. Huang, X. Kou, W. Cao, L. Li, L. Ge, J. Li, Ceram. Int. **43**,192 (2017).
[21] N. S. Nam, D. N. Khang, L. Q. Tuan, L. T. Son, Int. J. Env. Tech. Sci. **2**, 31 (2016).
[22] P. N. Manoudis, I. Karapanagiotis, A. Tsakalof, I. Zuburtikudis, B. Kolinkeová, C. Panayiotou, Appl. Phys. A **97**, 351 (2009).
[23] A. A. Widati, N. Nuryono, I. Kartini, AIMS Materials Science **6**(1), 10 (2019).
[24] E. Chitanu, T. Malaeru, M. M. Codescu, C. A. Banciu, V. Marinescu, 2021 12th International Symposium on Advanced Topics in Electrical Engineering (ATEE), 1 (2021),
[25] F. Cuoq, A. Masion, J. Labille, J. Rose, F. Ziarelli B. Prelot, J. Y. Bottero, Appl. Surf. Sci. **266**, 155 (2013).
[26] G. Tahereh, S.N. Masoud, B. Mehdi, Superlattices Microstruct. **61**, 33 (2013).
[27] N. H. N. Kamarudin, A. A. Jalil, S. Triwahyono, N. F. M. Salleh, A. H. Karim, R. R. Mukti, B. H. Hameed, A. Ahmed, Micropor. Mesopor. Mat. **180**, 235 (2013).

*Corresponding authors: elena.chitanu@icpe-ca.ro
cristina.banciu@icpe-ca.ro